Acta Universitatis Sapientiae
Electrical and Mechanical Engineering, 14 (2022) 1–12

DOI: 10.2478/auseme-2022-0001

Hydrodynamic Comparative Study on the Pumping Effects of a Square Tank Equipped with Single-Stage and Bi-Stage Impellers

Abdelghani BELHANAFI[1], Zied DRISS[2] and Mohamed Salah ABID[2]

[1] Department of Mechanical Engineering, Faculty of Mechanics,
University of Sciences and Technology of Oran Mohamed Boudiaf (USTO-MB),
El Mnaouer, PO Box 1505, Bir El Djir 31000, Oran, Algeria,
e-mail: abdelghani.belhanafi@univ-usto.dz
[2]National School of Engineers of Sfax (ENIS), Laboratory of Electro-Mechanic Systems (LASEM), B.P. 1173, km 3.5 Soukra, 3038 Sfax, Tunisia,
e-mail: Zied.Driss@enis.rnu.tn, MohamedSalah.Abid@enis.rnu.tn

Manuscript received January 03, 2022; revised November 26, 2022

Abstract: A computational fluid dynamics simulation is done for comparative study from the pumping effect on the four surfaces of the stirred tank. The flow field generated by one-stage and bi-stage six-bladed Rushton turbine in the unbaffled square tank was studied. The Reynolds-averaged Navier-Stokes equation with steady-state multi-reference frame approach (MRF) is used to simulate hydrodynamic flow in the tank. The turbulent viscosity, the turbulent kinetic energy and mean velocity distributions obtained in vertical and horizontal plans are analyzed and discussed. We can deduce that the additional Rushton turbine in the upper part of the square tank improves the quality of the mixture.

Keywords: Square tank, CFD, single-stage turbine, bi-stage turbines, agitation.

1. Introduction

Mechanical agitation is a process used for mixing miscible fluids, which has a wide field of application, like in the preparations of industrial, chemical, and pharmaceutical products; the stirring techniques are parameters to be taken into account during the implementation of these mixtures.

Many researchers have focused on the design of agitated tanks and impeller geometry. Pericleous and Patel [1] modeled radial impeller with one or more stages, on the basis of the relative velocity of the fluid and the drag coefficients taken from the literature. Taca and Paunescu [2] studied the influence of the shape of the reservoir on the evolution of the power number, for a closed spherical vessel equipped with a Rushton turbine, while the fluid contained solid particles in suspension. Guillard and Trägårdh (2003) designed and tested a new model for estimating mixing times in aerated three-reactor stirring tanks, equipped with two, three and four impellers. The results showed that the developed analogy model is independent of the scale, the geometry of the tank, the number of impellers used, the distance between the impellers and the degree of homogeneity considered. Murthy and Joshi [4] tested multiple impeller designs namely disc turbine, a variety of pitched blades varying in blade angle and hydrofoil impeller. Woziwodzki et al. [5] studied the mixing efficiency of shear-thinning fluids using carboxy methyl cellulose sodium salt (Na-CMC) aqueous solutions of varying mass concentrations and three types of impellers (Rushton turbine (RT), six-flat-blade turbine (FBT), six-pitched-down-blade turbine (PBT)) which were mounted on a common shaft in combinations of three, four, and five impellers. Vakili et al. [6] studied the effect of different geometric parameters in stirred vessels equipped with two blades impeller (FBT2). They employed steady-state approach MRF and standard k-ε turbulence model in their parametric study. Ammar et al. [7] compared the effect of the tank design on the hydrodynamic structure generated with a pitched blade turbine by realizing three types of configurations: a flat-bottomed cylindrical vessel, a dished bottomed cylindrical vessel, and a spherical vessel using a CFD code. A comparative study conducted by Jie et al. [8] on the design of tanks, flat bottom, and dished bottom equipped with a Rushton turbine on the distribution of velocity in a transitional and turbulent flow. They found that the shapes of the bottom tank have a significant effect on flow patterns as well as on the velocity profiles below the impeller. In recent years, solid particles and mass transfer characteristics on power consumption using multi-impeller in gas-liquid stirred tank reactors have been extensively studied by Zhang et al. [9]. Gong et al. [10] studied the effect of different geometric parameters in stirred vessels with a flat square base equipped with four blades impeller on the concentration of the particles in a solid-liquid system. A comparative study conducted by Weipeng et al. [11] between liquid-level height and particle distribution in unbaffled square stirred-tank reactors was done. They concluded that the height-to-width ratio of the tank might affect the distribution of suspended particles in the flocculating system. Another interesting investigation was performed by Weipeng et al. [11], [12] on the mobile type effect of agitation and its position in a baffled stirred-tank reactor. The used geometry is a square flat bottom tank equipped with four baffles placed at 90° with a distance ratio between the impeller and the bottom which varies between C= 0.20H (30 mm), 0.27H (40 mm), 0.33H (50 mm), and 0.40H (60 mm). They confirmed that the tank with a spherical shape provides uniform flow in the whole vessel volume. The experimental study performed by Deyin et al. [13] in a flat bottomed transparent cylindrical plexiglass tank equipped with four pitched-blade impellers was performed to evaluate the influence of the impeller speed, impeller type, and impeller spacing on the solid-liquid mixing process. The experimental study performed by Fabiana et al. [14] in a baffled square tank reactor equipped with four pitched blade turbines was performed to evaluate the influence of the impeller clearance. From these anterior studies, it is clear that the design investigation of the external shape for the stirred tank is very useful.

The present work aims to determine the influence of the external design of the tank on the hydrodynamic structure of the flow. Moreover, we are interested in adding the second impeller with radial pumping direction on the four vertical walls of square vessels equipped with six flat blade Rushton turbines (RT6).

2. Stirred Tank Configuration

The design and dimensions of the stirred tanks with Rushton impellers of standard geometry used in this work are represented in *Fig. 1*. The square tanks were filled with water up to a height of $H = T$; diameter and the height H are equal to 0.5 m. The first configuration was equipped with a six-bladed Rushton turbine with a diameter d equal to $T/3$. The offset of the impeller from the vessel bottom C was equal to $T/3$. In the second configuration, the spacing between the turbines RT6 is defined by $h_1 = h_2 = T/3$.

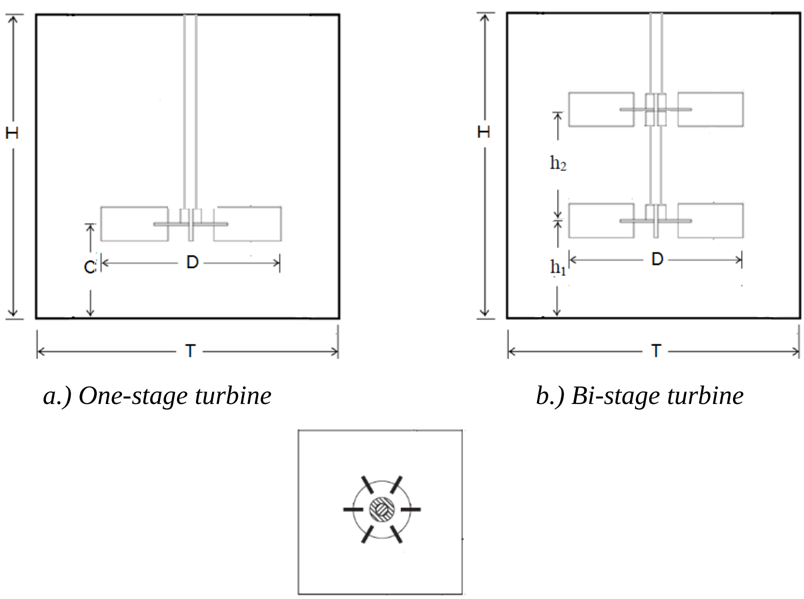

Figure 1: Mixing vessel dimensions: *a.* Single-stage turbine. *b.* Bi-stage turbine

3. Numerical Procedure

In the turbulent regime and for an incompressible fluid, the momentum equations were solved by using the finite volume method. A pre-processor was used to discretize the 3D flow domain with a tetrahedral mesh shown in *Fig. 2*. The computational domain is reduced to 180°, with three blades and half of the shaft from the tank with one stage impeller. Periodic conditions are imposed on all properties ensuring the continuity of the computational grid in the angular direction (θ = 90° and θ = -90°).

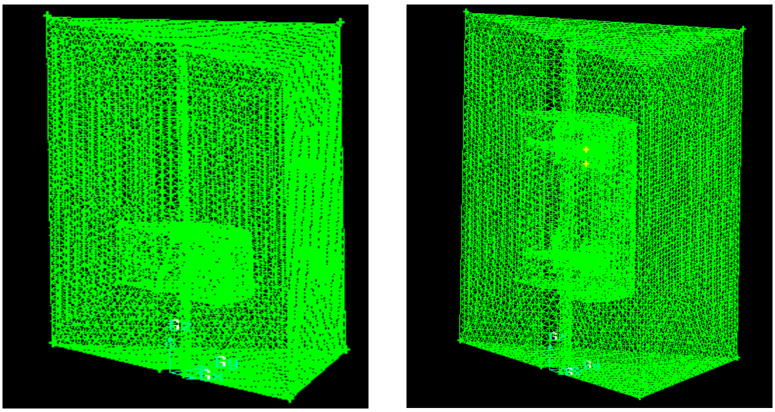

a.) Single-stage turbine *b.) Bi-stage turbine*

Figure 2: Tetrahedral mesh generation

The computational domain was divided into two blocks, the internal one containing the impellers and the external one containing the vessel walls for each case. The boundary conditions are introduced in the CFD code, using the multiple referential approaches (MRF). In this approach, the interface between the two regions is treated by the method called the frozen rotor. In this approach, the flow fields are connected at the interior surfaces (interface) separating the two domains by the method called the frozen rotor.

4. Mathematical Formulation

Governing Equations

The flow in a stirred vessel can be solved by the Navier-Stokes equations. The equations are written in their averaged form RANS (Reynolds Averaged

Navier Stokes) used in the case of a turbulent flow, due to the time of the turbulence scales.

The continuity equation is written as follows:

$$\frac{\partial \rho}{\partial t} + \nabla\left(\rho \vec{u}\right) = 0 \tag{1}$$

ρ is the density, *t* is the time and *u* is the velocity vector.

The momentum equation is written as follows:

$$\frac{\partial}{\partial t}\left(\rho \cdot \vec{u}\right) + \nabla\left(\rho \cdot \vec{u} \cdot \vec{u}\right) = -\nabla p + \nabla \tau + \vec{F} \tag{2}$$

τ is the shear stress given by:

$$\tau = -p \cdot \delta + \mu \cdot \left(\nabla \vec{u} + \left(\nabla \vec{u}\right)^{T}\right) \tag{3}$$

For each species, the form equation can be written as follows:

$$\frac{\partial \rho \cdot c}{\partial t} + \nabla\left(\rho \cdot \vec{u} \cdot c\right) = \nabla\left(D \cdot \nabla c - \rho \cdot \overline{c' \cdot u'}\right) + R \tag{4}$$

where *c* is the species concentration, *D* is the laminar diffusion coefficient and *R* represents the terms due to reactions.

For the turbulent Modeling, we have used the standard *k*-*ε* model based on the following two equations:

$$\frac{\partial \rho \cdot k}{\partial t} + \nabla\left(\rho \cdot \vec{u} \cdot k\right) = \nabla\left[\left(\mu + \frac{\mu_t}{\sigma \cdot k}\right) \cdot \nabla k\right] = P - \rho \cdot \varepsilon \tag{5}$$

$$\frac{\partial \rho \cdot \varepsilon}{\partial t} + \nabla\left(\rho \cdot \vec{u} \cdot \varepsilon\right) = \nabla\left[\left(\mu + \frac{\mu_t}{\sigma \cdot \varepsilon}\right) \cdot \nabla \varepsilon\right] = C_1 \cdot \frac{\varepsilon}{k} \cdot P - C_2 \cdot \frac{\varepsilon^2}{k} \tag{6}$$

These equations represent the conservation of the turbulent kinetic energy *k* and the dissipation rate of the turbulent kinetic energy ε respectively. In the above equations, the quantity *P* is the production of kinetic energy, which is calculated from:

$$P = \mu_{eff} \cdot \nabla \vec{u} \cdot \left(\nabla \vec{u} + \left(\nabla \vec{u}\right)^{T}\right) \tag{7}$$

The effective viscosity is defined as follows:

$$\mu_{eff} = \mu + \mu_t \tag{8}$$

μ_t is the turbulent viscosity, it is defined as follows:

$$\mu_t = C_\mu \cdot \rho \cdot \frac{k^2}{\varepsilon} \tag{9}$$

Equations (5) and (6) are based on exact equations and reveal required constants to model the turbulence. The "standard" constant values are:

$$C_\mu = 0.09, \quad C_1 = 1.44, \quad C_2 = 1.92, \quad \sigma_k = 1.0, \quad \sigma_\varepsilon = 1.3. \tag{10}$$

5. Numerical Results

5.1 Comparison with Experimental Results

Fig. 3 illustrates the predicted axial profile of the dimensionless radial velocity component with a Rushton turbine. With the exactly same geometrical conditions, we predicted the variation of the axial velocity along the stirred vessel. The comparison between our results and those given experimentally by Montante et al. [15] shows good agreement.

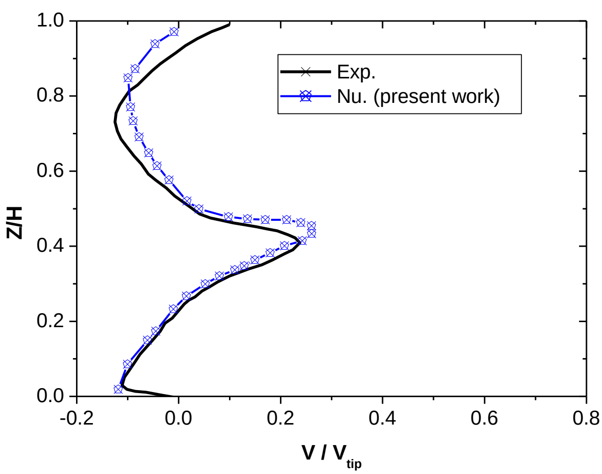

Figure 3: Axial profiles of the dimensionless radial velocity, N=240 rpm

5.2 Results and Discussion

5.2.1 Turbulent Viscosity

The horizontal presentation planes of turbulent viscosity distribution is illustrated in *Fig. 4* for both geometries at the central part of the vessel with

z/H = 0.5. In one stage system, the large zone of turbulent viscosity is extended throughout the volume of the tank (*Fig. 4a*). But in the second configuration, the maximum values of the turbulent viscosity are located at the shaft of the agitator (*Fig. 4b*). At the proximity of the four sidewalls of the square tanks, the turbulent viscosity drops rapidly. However, the stirring effect is still much more intense in the plane above the turbine in the first configuration (*Fig. 4a*). The turbulent viscosity is maximum in the vessel equipped with a bi-stage turbine with a 7.06 Pa·s value (*Fig. 4b*).

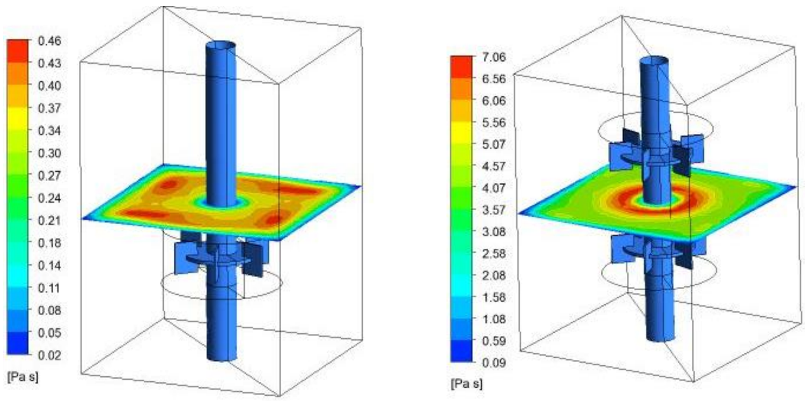

a.) Single-stage turbine *b.) Bi-stage turbine*

Figure 4: Turbulent viscosity contours in the r- θ plane

The turbulent viscosity generated for both cases is presented in *Fig. 5*. From these results, it is found that the position of the maximum values of turbulent viscosity is obtained at the tank with bi-stage impellers. Within one impeller system, the distribution of the turbulent viscosity is developed in the interior and superior part of the tank (*Fig. 4a*). Another remark for the second configuration (*Fig. 5b*), is that the turbulent viscosity is concentrated in space between two turbines caused a number of stages. According to these results, it is noted that the maximum value of the turbulent viscosity is obtained within two impeller stages is 6.73 Pa·s.

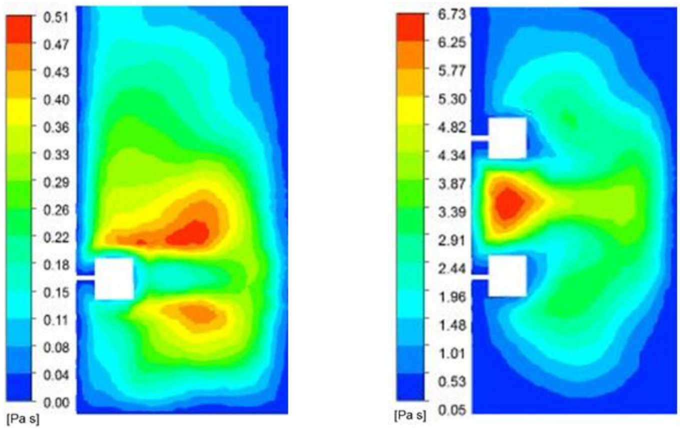

a.) Single-stage turbine *b.) Bi-stage turbine*

Figure 5: Turbulent viscosity contours in the *r*-*z* plane

5.2.2 Mean Velocity Distribution

5.2.2.1 Single Stage and Bi-stage Turbine in Vertical Plane

The mean velocity field produced by the Rushton turbine from the two configurations in the vertical plane is shown in *Fig. 7*. Globally, in the domain swept by the turbine blades, the velocity remains elevated enough. Within two impeller systems, the distribution of the mean velocity is developed throughout the volume of the square tank (*Fig. 6b*). Contrary to the tank with one-stage, in the upper part of the square vessel the mean velocity is very low (*Fig. 6a*). In the bi-stage vessel, the mean velocity obtained had an optimal value of 6.59 m/s. In a square tank, the use of the bi-Rushton turbines is more advantageous and increases the mean velocity.

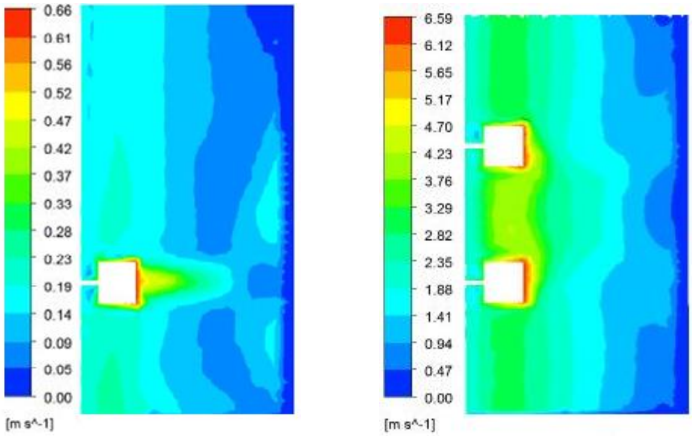

a.) Single-stage turbine *b.) Bi-stage turbine*

Figure 6: Mean velocity contours in the *r-z* plane

5.2.3 Radial Profiles

Three different axial positions were chosen for velocity and turbulent kinetic energy dimensionless for the two configurations at an angular position equal to $\theta = 0°$ following: from the half-width of the blade (r = 0.07 m), at the blade tip (r = 0.085 m) and just near the leading edge of the turbine blade (r = 0.1 m).

5.2.3.1 Turbulent Kinetic Energy

The profiles plotted in *Fig. 7* give the distribution of dimensionless turbulent kinetic energy for two cases at different axial positions, and are presented along the vessel radius. According to these results, it is noted that the maximum value of the kinetic energy is obtained within the bi-stage system. We can see that the region of the maximum values (k*> 0.075) is located in the wake which develops at the mid-width of the blade (r = 0.07 m). Another point, which can be underlined, is that the increase in the number of Rushton turbines in a square tank yields higher radial pumping speed. For a location just near the region swept by the blade corresponding to (r = 0.1 m), the turbulent kinetic energy is dominated by maximum values in the first configuration. Outside of this area at (r = 0.07 m and r = 0.085 m), the low values of the turbulent kinetic energy are present (*Fig. 7a*). Thus, to ensure agitation in the whole square vessel volume, it is necessary to add a second turbine.

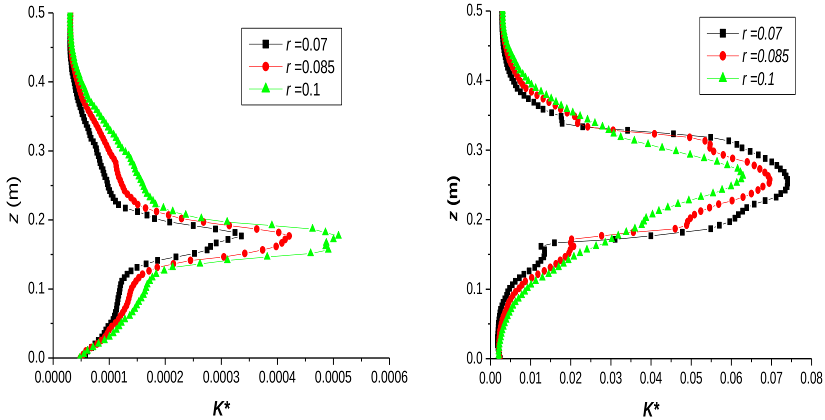

a.) Single-stage turbine *b.) Bi-stage turbine*

Figure 7: Radial profiles of the turbulent kinetic energy for different blade positions (r = 0.07 m, 0.085 m, 0.1 m)

5.2.3.2 Tangential Velocity

The dimensionless tangential velocity is plotted in *Fig. 8* for the two cases studied with different axial positions, represented along the vessel radius. For the first case where just one impeller is used located at the height $z/H = 0.33$ of the vessel, the tangential circulation can't reach the free surface. At mid-width blade ($r = 0.07$ m) the optimum velocity obtained for a bi-stage tank is $W/V_{tip} = \pm 0.45$. For any case studied, the minus sign of velocity indicates the existence of a recirculation flow. The low values of dimensionless tangential velocity are obtained at ($r = 0.1$ m) in the area swept by one impeller (*Fig. 8a*). In *Fig. 8b*, we remark that the chaotic regions produced between impellers are intensified for the second case, giving better performance. If another impeller is added at the upper part of the square vessel, that can ensure mixing at this space.

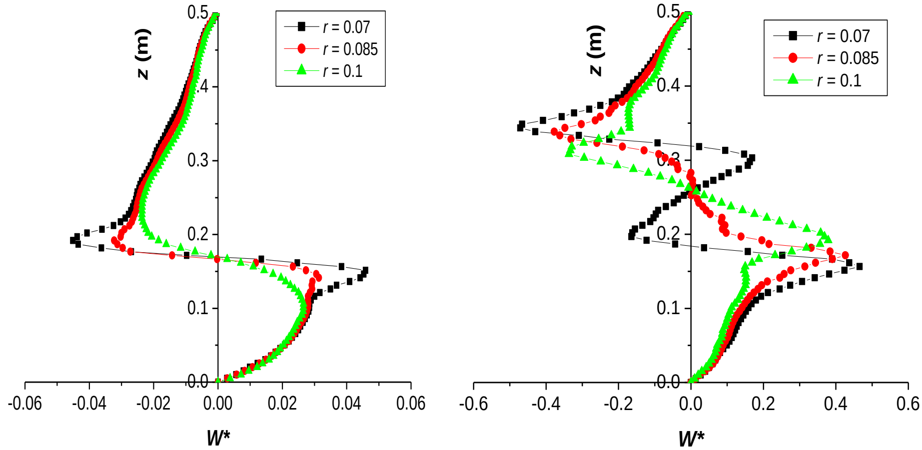

Figure 8: Radial profiles of the tangential velocity for different positions of the blade (r = 0.07 m, 0.085 m, 0.1 m)

6. Conclusion

The aim of the investigation in this work was to determine the effect of adding the second Ruston turbine with radial pumping direction on the four vertical walls of the square vessel. From the presented results the following conclusions can be deduced:

Within one stage Rushton turbine, the shape of the wake of turbulent viscosity is more extended in the upper part of the square tank. Contrary to the square tank with bi-stage Rushton turbines, the turbulent viscosity is concentrated in the space between two impellers. For the two planes just below and above the Rushton turbine, a large zone of maximum velocity is extended to the solid walls in a square tank equipped with a single impeller. As can be deduced, for a bi-stage system the typical double loop flow circulation of tangential velocity is apparent throughout the volume of the square tank. This dynamic phenomenon is absent in the square stirred vessel with a single Rushton turbine. The increased number of impellers RT6 in a square tank plays an important role by improving the operating conditions of stirring and mixing. We can conclude that, the use of the bi-Rushton turbine at axial position z/H = 0.66 in the square tank is more advantageous than one stage turbine and increases the performance of agitation operation.

References

[1] Pericleous, K.A. and Patel, M.K., “The modelling of tangential and axial agitators in chemical reactors”, *Physico. Chem. Hydrodyn.*, 8, pp. 105–123, 1987.

[2] Taca, D.C. and Paunescu, M., “Power input in closed stirred vessels”, *Chemical Engineering Science.*, 56, pp. 4445–4450, 2001.

[3] Guillard, F. and Trägardh, C., “Mixing in industrial Rushton turbine agitated reactors under aerated conditions”, *Chemical Engineering and Processing.*, 42, pp. 373-386. 2003.

[4] Murthy, N.B. and Joshi, J.B., Assessment of standard k-ε, RSM and LES turbulent models in a baffled stirred agitated by various impeller designs”, *Chemical Engineering Science.*, 63, pp. 5468–5495, 2008.

[5] Woziwodzki, S., Broniarz, P.L. and Ochowiak, M., “Transitional mixing of shear-thinning fluids in vessels with multiple impellers”, *Chemical Engineering and Technology.*, 33(7), pp. 1099–1106, 2010.

[6] Vakili, M.H., Nasir, M. and Esfaharry, B., “CFD analysis of turbulence in a baffled stirred tank, a three-compartment model”. *Chem. Eng. Sci*., 64, pp. 351-362, 2009.

[7] Ammar, M., Driss, Z., Chtourou, W. and Abid, M. S., “Effect of the Tank Design on the Flow Pattern Generated with a Pitched Blade Turbine”. *International Journal of Mechanics and Applications*., 2(1), pp. 12–19, 2012.

[8] Jie, D., Binjie, H., Andrzej, W. P., Xiaogang, Y. and Nicholas, J. M., “The Effect of bottom shape and baffle length on the flow field in stirred tanks in turbulent and transitional flow”, *International Journal of Mechanical*., 10(9), pp. 10005417, 2016.

[9] Zhang, J., Zhengming G., Yating, C., Huayu, C., Ziqi, C. and Yuyun, Bao., “Power consumption and mass transfer in a gas-liquid-solid stirred tank reactor with various triple-impeller combinations”, *Chemical Engineering Science*., 170, pp. 464–475, 2017.

[10] Gong, H., Huang, F., Li, Z., Gao, Z. and Derksen, J. J., “Mechanisms for drawdown of floating particles in a laminar stirred tank flow”, *Chemical Engineering Journal.*, 346, pp. 340-350, 2018.

[11] Weipeng, H., Lianpeng, X., Beata, G., Jun, N. and Zhou, S., “Comparative analysis on flocculation performance in unbaffled square stirred tanks with different height-to-width ratios: Experimental and CFD investigations”, *Chemical Engineering Research and Design.*, 132, pp. 518–535, 2018.

[12] Weipeng, H., Zhoulong, X., Ziyue, Z., Maolin, H. and Mengmeng, Pan., Effect of impeller clearance on floc growth behaviors in a baffled square stirred-tank reactor, *Separation and purification technology*., 212, pp. 233–244, 2019.

[13] Deyin, G., Chao, C., Zuohua, L. and Yundong, W., “Numerical simulation of solid-liquid mixing characteristics in a stirred tank with fractal impellers”, *Advanced Powder Technology*., 30, pp. 2126–2138, 2019.
Fabiana M. B. Coelho, A. M. Botelho, O.F. Ivo, F. I. Priscilla, F. F. A, Tatiana F. F, “Volumetric mass transfer coefficient for carbon monoxide in a dual impeller stirred tank reactor considering a perfluorocarbon–water mixture as liquid phase”, *Chemical Engineering Research and Design.*, 143, pp. 160–169, 2019.

[14] Montante, G and Magelli, F., “Liquid homogenization characteristics in vessels stirred with miltiple Rusthton turbines mounted at different spacings, CFD study and comparison with experimental data”, *Chemical Engineering Research and Design*, 82 (A9), pp. 1179–1187, 2004.